frontiers | Frontiers in Chemical Engineering

TYPE Original Research
PUBLISHED 10 April 2024
DOI 10.3389/fceng.2024.1342755

Check for updates

OPEN ACCESS

EDITED BY
Kavitha S.,
Karpagam Academy of Higher Education, India

REVIEWED BY
Yongfei Xue,
Central South University of Forestry and Technology, China
Pooja Sharma,
National University of Singapore, Singapore

*CORRESPONDENCE
Antonio Pereira,
apereira@ufpa.br

RECEIVED 22 November 2023
ACCEPTED 14 March 2024
PUBLISHED 10 April 2024

CITATION
Fonseca SSSd, Rodrigues TDVP, Pinheiro WBdS, Teixeira EB, dos Santos KIP, da Silva MGdOP, de Sousa AM, do Vale DMC, Pinho JD, Araújo TMT, Khayat AS and Pereira A (2024), The effect of 1-deoxynojirimycin isolated from logging residue of *Bagassa guianensis* on an *in vitro* cancer model.
Front. Chem. Eng. 6:1342755.
doi: 10.3389/fceng.2024.1342755

COPYRIGHT
© 2024 Fonseca, Rodrigues, Pinheiro, Teixeira, dos Santos, da Silva, de Sousa, do Vale, Pinho, Araújo, Khayat and Pereira. This is an open-access article distributed under the terms of the Creative Commons Attribution License (CC BY). The use, distribution or reproduction in other forums is permitted, provided the original author(s) and the copyright owner(s) are credited and that the original publication in this journal is cited, in accordance with accepted academic practice. No use, distribution or reproduction is permitted which does not comply with these terms.

The effect of 1-deoxynojirimycin isolated from logging residue of *Bagassa guianensis* on an *in vitro* cancer model

Susanne Suely Santos da Fonseca[1,2], Thaíssa Vitória Portal Rodrigues[2], Wandson Braamcamp de Souza Pinheiro[3], Eliel Barbosa Teixeira[2], Kyouk Isabel Portilho dos Santos[3], Marcelli Geisse de Oliveira Prata da Silva[2], Amanda Marques de Sousa[2], Débora Monteiro Carneiro do Vale[4], Jaqueline Diniz Pinho[2], Taíssa Maíra Thomaz Araújo[2], André Salim Khayat[2] and Antonio Pereira[1]*

[1]Institute of Technology, Federal University of Pará, Belém, Pará, Brazil, [2]Oncology Research Center, Federal University of Pará, Belém, Pará, Brazil, [3]Central Extraction Laboratory, Chemistry Graduate Program, Federal University of Pará, Belém, Pará, Brazil, [4]Molecular Biology Laboratory, Ophir Loyola Hospital, Belém, Pará, Brazil

Introduction: *Bagassa guianensis* Aubl, a tree widely distributed in Brazil, significantly contributes to the furniture industry. Notably, it harbors the bioactive compound 1-deoxynojirimycin (1-DNJ), which is retrievable from timber residues and retains activity even days after wood extraction. This makes *Bagassa guianensis* a promising biological resource for anticancer therapy and pharmacology studies. This study delves into the *in vitro* antineoplastic actions of 1-DNJ, focusing on adenocarcinoma gastric cell lines (ACP02) and glioblastoma (A172).

Methods: The effect of 1-DNJ on cell viability was evaluated after 72 hours of treatment in the ACP02 and A172 cell lines. We also assessed the effect of 1-DNJ on the pattern of cell migration, cell death, changes in the cell cycle by flow cytometry, the production of reactive oxygen, and its antioxidant capacity in the scavenging of free radicals.

Results: Assessing cell viability after 72 h (about 3 days) of treatment reveals a remarkable reduction, particularly in glioblastoma cells (A172), exhibiting a lower IC50 compared to ACP02 and MRC5 (fibroblast derived from normal lung tissue) cell lines. This decreased viability correlates with reduced reactive oxygen species (ROS) production in both cell lines after the treatment with 1-DNJ. Furthermore, 1-DNJ induces cell cycle arrest, impedes cell migration, and prompts cell death in ACP02 and A172.

10.3389/fceng.2024.1342755

Discussion: These findings support 1-DNJ as a potent antineoplastic agent, particularly efficacious against glioblastoma and gastric adenocarcinoma. Thus, unveiling the therapeutic potential of *Bagassa guianensis* Aubl for cancer treatment and expanding the horizons of bioeconomy applications.

KEYWORDS

antineoplastic, 1-deoxynojirimycin, gastric adenocarcinoma, glioblastoma multiforme, oxidative stress, bioeconomy, bioactive compound, *Bagassa guianensis*

1 Introduction

The unparalleled biodiversity of the Amazon is under threat due to indiscriminate logging, which contributes to deforestation and puts numerous plant species at risk (Brancalion et al., 2018). In contrast, sustainable forest management not only supports local economies but also paves the way for adopting a circular bioeconomy in the region (McDermott et al., 2015; Watanabe et al., 2018), benefiting a wide array of stakeholders including indigenous populations and eco-friendly businesses. Selective logging, a prominent practice in legal logging, entails the careful selection of certain trees for harvest, thus minimizing waste and promoting more responsible use of resources (Asner et al., 2005; Acquah et al., 2016). One such tree, Bagassa guianensis Aubl or Tatajuba, is abundant in Brazil's North and Northeast, especially in states like Pará and Maranhão. Notably, its timber waste, often left to decay, contains bioactive compounds such as 1-deoxynojirimycin (1-DNJ), which has been identified to linger in the wood residues (Pinheiro et al., 2022). While 1-DNJ is also present in Morus sp. leaves, silkworm parts, and produced by bacteria like *Bacillus* velezensis, these sources do not yield the compound as abundantly (Yin et al., 2010; Parida et al., 2019; Lee et al., 2021; Marchetti et al., 2021).

This study zeroes in on 1-DNJ extracted from Tatajuba's timber waste, exploring its potential anticancer effects. Previous research has established 1-DNJ's antioxidant and anti-inflammatory capabilities, suggesting its suitability for anticancer therapy (Naik et al., 2015; George et al., 2017; Nyambe et al., 2019). For example, Morus nigra extract, rich in 1-DNJ, has been shown to have such effects and to inhibit carcinogenesis in prostate cancer models and prevent gastric ulcers in mice (Yatsunami et al., 2008; Turan et al., 2017; Piao et al., 2018). Given the significant global impact of cancer, with 19.3 million new cases and nearly 10 million deaths in 2020 alone (Bray et al., 2021; Sung et al., 2021), it is imperative to develop new therapeutic strategies to improve patient survival rates (Bray et al., 2021)."

2 Materials and methods

2.1 Isolation of 1-deoxynojirimycin from the plant *Bagassa guianensis* Aubl

To isolate 1-deoxynojirimycin, 500 g of Bagassa guianensis Aubl stem bark residue, sourced from sustainable forestry practices, was utilized. The dried and finely milled biomass, supplied by the Central Extraction Laboratory of the Federal University of Pará, underwent ultrapure water extraction. This process was performed in an ultrasonic bath (BRANSON 2510 – Danbury, CT, USA) set to a frequency of 42 kHz, a power of 100 W, and a stable temperature of 27°C, ensuring optimal extraction without thermal degradation. The biomass was exposed to the ultrasonic waves in a sealed container with indirect contact for 30 min. The resulting extract was filtered through a fine mesh to remove particulates, and the extraction was repeated twice more, yielding three cumulative batches. These extracts were then combined and concentrated using a rotary evaporator under reduced pressure at a controlled temperature to preserve the integrity of the volatile components, resulting in 50g of a crude dry extract. Fractionation of the crude extract was accomplished through wet column chromatography (WCC), utilizing silica as the stationary phase. A solvent system of acetone and methanol in a 1:1 ratio was chosen for its efficacy in separating the desired compound, which was confirmed by passing the mixture through the column twice. To finalize the isolation, pure methanol, known for its high elution strength, was used to elute the substance from the silica. The fraction containing 1-deoxynojirimycin was then air-dried in a fume hood, affording 10g of the purified substance. The molecular structure of the isolated compound was confirmed by 1H e 13C Nuclear Magnetic Resonance (NMR) spectroscopy (Figure 1). The NMR spectra were recorded and analyzed, providing definitive structural identification consistent with known data for 1-deoxynojirimycin, thus validating the isolation process.

2.2 Identification and purity analysis of 1-Deoxynojirimycin

For the structural identification and purity assessment of 1-deoxynojirimycin (compound S1), 1H and 13C Nuclear Magnetic

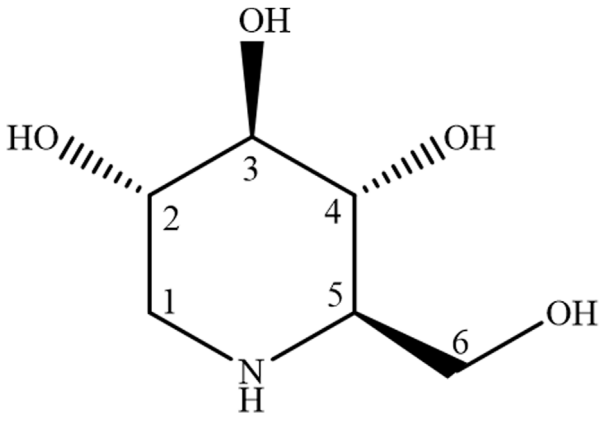

FIGURE 1
Structural formula of 1-deoxynojirimycin.

Resonance (NMR) spectra were acquired. We utilized a Bruker Ascend™ spectrometer operating at 400 MHz for 1H NMR and 100 MHz for 13C NMR (Germany). Preparation involved dissolving 50 mg of S1 in 600 μL of deuterated water (D2O), with the subsequent data control and processing by TopSpin software (Version 3.6.0). The Free Induction Decays (FIDs) were transformed using Fourier transform, applying a line broadening (LB) of 0.3 Hz to enhance resolution. Residual D2O signal suppression was achieved through low power pre-saturation sequences, and manual adjustments were made for baseline correction and calibration. The residual solvent peak at 4.82 ppm in D2O provided an internal reference for calibration.

The physical form of compound S1 was noted as a brown to red solid with solubility in H2O. It was isolated via counter-current chromatography (CCC) following ultrasonication of the aqueous extract. The 1H NMR spectrum (Supplementary Material S1) displayed eight distinct signals in the δH 3.0 to 4.0 range, consistent with single hydrogen integrations. Analysis of these chemical shifts and coupling constants suggested these hydrogens were linked to an oxymethine carbon or in proximity to a heteroatom, as detailed in Supplementary Table A. Corroborating this, the 13C NMR spectrum (Supplementary Material S2) exhibited six lines between δC 45.0 and 80.0, indicative of a cyclic saccharide structure. Cross-referencing the spectral data from 1H and 13C NMR with established literature values (Pinheiro et al., 2022), the molecular identity of compound S1 was confirmed as the iminosugar 1-deoxynojirimycin.

2.3 Cell cultures

Cells were seeded in 96-well microplates at a density optimized for each cell line to ensure uniform growth and responsiveness. The cell lines used included A172 (grade IV astrocytic tumor/glioblastoma multiforme), provided by the Clinical Cytopathology Laboratory at the School of Pharmaceutical Sciences, Federal University of São Paulo. The primary gastric adenocarcinoma cell line ACP02 was developed and established by the Human Cytogenetics Laboratory, Federal University of Pará (UFPA) (Leal et al., 2009). Additionally, the MRC5 cell line (human lung fibroblast) from the Oncology Nucleus of UFPA was included as a non-neoplastic culture model. For cell culture, aseptic techniques such as laminar flow work and sterile handling were strictly adhered to. The ACP02 cell line was cultured in Dulbecco's Modified Eagle's Medium F12 (DMEM-F12), while the A172 and MRC5 cell lines were maintained in DMEM medium. The media for all cell lines were enriched with 10% fetal bovine serum (FBS) and supplemented with 1% antibiotic and antimycotic solution (Gibco) to prevent microbial contamination. Cultures were kept in a humidified incubator set to an atmosphere of 95% air and 5% CO2 at a constant temperature of 37°C. Confluence was carefully monitored, with experiments initiated upon reaching 70%–80% confluence to ensure cells were in the exponential phase of growth. The integrity of the cell lines was regularly verified through genetic profiling, and routine *mycoplasma* testing was conducted to confirm the absence of contamination. These stringent protocols guaranteed that the results could be confidently attributed to the biological properties of the cells.

2.4 Cell viability and selectivity index

For the cytotoxicity assay, the MRC5 and ACP02 cell lines were seeded in 96-well plates at a density of 3×10^4 cells per well, while the A172 cell line was seeded at a higher density of 5×10^4 cells per well to account for its distinct growth kinetics. The cells were treated with varying concentrations of 1-DNJ, ranging from 0.5 to 32 mM, prepared in a 0.01% DMSO solution, selected for its inert properties and ability to dissolve 1-DNJ effectively without affecting cell viability. Each cell line was maintained in its optimal medium, with DMEM/F12 for the ACP02 and MRC5 cell lines, and DMEM for the A172 cells, both supplemented with 5% Fetal Bovine Serum. The incubation took place in a CO2 incubator set at 37°C with a 5% CO2 atmosphere for 72 h, conditions conducive to cell growth and response to treatment.

The cell viability post-treatment was assessed using the 3-(4,5-dimethylthiazol-2-yl)-2,5-diphenyltetrazolium bromide (MTT) assay, a colorimetric method where the reduction of MTT to formazan by metabolically active cells is measured. After incubation with the MTT reagent, the formazan product was solubilized, and the absorbance at 570 nm was measured using a microplate spectrophotometer, with the DMSO-only wells serving as blanks. The selectivity index of 1-DNJ was calculated by determining the ratio of IC50 values in the normal MRC5 cell line to the IC50 and IC25 in the A172 and ACP02 cancer cell lines, using non-linear regression analysis. An index of 3 or greater, as suggested by Indrayanto et al. (2021), is indicative of a favorable selectivity profile, suggesting that 1-DNJ is more toxic to cancer cells than to normal cells, which is essential for the potential therapeutic application of the compound.

2.5 Cell cycle assessment by flow cytometry

Cells were plated in 12-well culture plates, designed for optimal cell attachment and growth, at a density of 1×10^6 cells per well. After a 24-hour period allowing for cell adherence and stabilization, the cultures were treated with 1-DNJ at precise concentrations determined by preliminary dose-response curves: 9.6 and 19.3 mM for the gastric cancer cell line ACP02, and 2.6 and 5.3 mM for the glioblastoma cell line A172. These concentrations represent the IC25 and IC50 values, respectively, aiming to evaluate a range of inhibitory effects. Control groups were maintained in parallel, with untreated cells receiving only the standard culture medium, which was DMEM supplemented with 5% fetal bovine serum, ensuring consistent conditions across all experimental setups. After a 72-hour incubation at 37°C in a CO2 incubator, providing an environment conducive to cell viability, the cultures were gently washed with phosphate-buffered saline (PBS) to remove any non-adherent cells and metabolic byproducts. Subsequently, cells were trypsinized using a 0.25% trypsin-EDTA solution to detach them for subsequent analysis. The cell suspension was then neutralized with an equivalent volume of culture medium and cells were stained with 50 μg/mL propidium iodide for at least 12 h to label the DNA of compromised cells, facilitating their identification during flow cytometry. Flow cytometric analysis was conducted on the BD FACSVerse™ system, processing ten thousand events per sample to ensure a robust representation of the cell population. Each group

consisted of four biological replicates, a number chosen to balance the need for statistical power with practical considerations of assay throughput and resource allocation, as proposed by Shahrestanaki et al. (2019). This sample size is adequate to detect significant differences between treated and control groups while accounting for biological variability.

2.6 Differential staining assay for the quantitative analysis of apoptotic and necrotic cells using ethidium bromide and acridine orange

In this assay, ACP02 and A172 cell lines were plated at a density of 1×10^5 cells per well in 12-well culture plates, with each well containing an appropriate volume of culture medium to sustain cell growth. After a 24-hour incubation period at 37°C in a 5% CO2 atmosphere, allowing for cell attachment and stabilization, the cells were treated with 1-DNJ. The concentrations of 9.6 and 19.3 mM for ACP02 and 2.6 and 5.3 mM for A172 were selected based on their respective IC50 values determined from previous dose-response studies. The cells were treated in triplicate wells for 72 h, a duration chosen to encompass at least one complete cell cycle. Post-treatment, the supernatant was carefully aspirated, and the cells were gently centrifuged at 1,000 rpm for 5 min, a speed and duration optimized to pellet the cells without disrupting their integrity. The supernatant was discarded, and the cell pellet was resuspended in 15 µL of PBS to ensure a suitable concentration for downstream analysis. For the dual staining, 1 µL of ethidium bromide/acridine orange solution was added directly to the cell suspension. This staining solution was prepared according to a standardized protocol to achieve consistent staining quality across all samples. A slide was then prepared for analysis under a fluorescence microscope equipped with the appropriate filters and at a magnification that allows clear differentiation of cellular phenotypes. A systematic counting of 300 cells from each sample was performed to quantify the percentage of each cellular phenotype: viable, apoptotic, and necrotic. The count of 300 cells was determined to provide a balance between a comprehensive assessment and a manageable workload for analysis. This sample size was deemed sufficient to detect significant trends in cell death patterns and is representative of the cell population's response to the treatment.

2.7 Cell migration assay using the wound healing test

The wound healing assay was conducted to assess the migratory response of ACP02 and A172 cancer cell lines to 1-DNJ treatment. Cells were seeded at a density of 2×10^5 cells per well in 12-well culture plates and grown to full confluence. A uniform scratch was introduced across the cell monolayer using a sterile pipette tip. Following the scratch, wells were rinsed with pre-warmed culture medium to remove cell debris and to standardize the initial condition of the cell-free gap. Each well was then treated with 1-DNJ at tailored concentrations specific to each cell line: 19.3 mM and 9.6 mM for ACP02, and 5.3 mM and 2.6 mM for A172. Parallel control wells contained culture medium without the drug. The migration of cells into the scratch area was monitored at 0 (immediately post-treatment), 6, 12, 24, 36, and 48 h using time-lapse photography on an inverted microscope with consistent magnification and focus. Quantitative analysis of the migration was performed using ImageJ software. The "scratch" area was measured at each time point, and the rate of area closure was calculated, providing an index of migratory speed for treated and control cultures. This allowed for a comparative evaluation of the anti-migratory potential of 1-DNJ on the cancer cell lines.

2.8 Quantitative evaluation of superoxide anion production in 1-DNJ treated cell lines using the NBT assay

To quantitatively assess the intracellular superoxide anion production, the Nitro Blue Tetrazolium (NBT) reduction assay was utilized following the methodology of Hyung et al. (2006). In this assay, a 1 mg/mL NBT solution was freshly prepared under light-protected conditions. This yellow solution undergoes a reduction reaction with intracellular superoxide radicals (O2-), forming a purple formazan precipitate. After treating the ACP02 and A172 cell lines with 1-DNJ at 19.3 and 9.6 mM, and 5.3 and 2.6 mM concentrations respectively for 72 h, cultures were washed with PBS and incubated with the NBT solution for 2 h at 37°C in the dark. Post-incubation, the medium was aspirated, cells were rinsed with PBS, and fixed rapidly with methanol. The cell membrane was then permeabilized using 2 M potassium hydroxide to facilitate the dissolution of formazan crystals. DMSO was added to fully solubilize the crystals, enabling quantitative analysis. Absorbance was measured at 620 nm using a microplate spectrophotometer, a wavelength optimal for detecting the reduced form of NBT. The absorbance readings provided a comparative measure of superoxide anion production between 1-DNJ treated and control cell lines, offering insights into the oxidative stress response induced by the treatment.

2.9 ABTS•$^+$ antioxidant ability

The scavenging activity of 1-DNJ against ABTS•$^+$ cation radicals was assessed, and the data were obtained through spectrophotometry using the SpectraMax i3 ELISA reader. To prepare the ABTS•$^+$ solution, an aqueous solution of diammonium salt 2,2′-Azino-bis(3-ethylbenzothiazoline-6-sulfonic acid) (ABTS•$^+$) (7 mM) was reacted with an aqueous solution of 140 mM potassium persulfate, following the procedure by Sridhar and Charles (2019). After 16 h of reaction, the solution was utilized for the tests. The antioxidant capacity of 1-DNJ was determined based on the reduction in absorbance at concentrations spanning 10–1,000 µM of 1-DNJ and the standard antioxidant Trolox, also at the same concentrations. The value was measured with the ABTS solution after 16 h of reaction. The mixture underwent incubation in the dark for 10 min, and absorbances were determined at a wavelength of 734 nm.

2.10 DPPH• antioxidant ability

The antioxidant efficacy of 1-DNJ against ABTS•$^+$ cation radicals was evaluated using a spectrophotometric assay, with readings taken by the SpectraMax i3 ELISA reader (Akar et al., 2017). The ABTS•$^+$ working solution was prepared by mixing a 7 mM aqueous solution of ABTS•$^+$ diammonium salt with a 140 mM potassium persulfate solution, as per the protocol by Sridhar and Charles (2019). This reaction mixture was then allowed to stand for 16 h at room temperature in the dark to generate the ABTS•$^+$cation radicals. The antioxidant capacity of 1-DNJ was quantified by its ability to reduce the absorbance of the ABTS•$^+$ solution, indicative of scavenging activity. A series of 1-DNJ concentrations ranging from 10 to 1,000 μM were tested against a standard curve of the known antioxidant Trolox, prepared at identical concentrations for comparative purposes. After adding 1-DNJ to the ABTS•$^+$ solution and incubating for 10 min in the dark to allow for reaction, the absorbance was measured at 734 nm. This wavelength is specifically selected for its sensitivity to the characteristic blue-green color of the ABTS•$^+$ cation, which diminishes upon reduction by an antioxidant. A decrease in absorbance relative to the control indicates the scavenging capability of 1-DNJ. The results are expressed in Trolox equivalent antioxidant capacity (TEAC), facilitating the comparison of 1-DNJ's antioxidant power to that of a well-established reference compound.

The antioxidant capacity of 1-DNJ was evaluated by the DPPH• radicals (1,1-diphenyl-2-picrylhydrazyl), and samples were quantified using a 96-well microplate spectrophotometer. In this assay, a 120 mM solution of DPPH• was prepared, serving as the DPPH• standard curve with concentrations ranging from 0 to 60 μM, following the methodology by Sridhar and Charles, 2019. A Trolox solution was also employed as a standard at 10–1,000 μM concentrations. 1-DNJ was diluted in an aqueous solution at concentrations spanning from 10 to 1,000 μM. Methanol and water were used as the reaction blank, and positive controls included 1-DNJ/water, DPPH•/methanol, and Trolox/methanol. The various concentrations of 1-DNJ and Trolox underwent a 30-minute incubation in the dark at room temperature. After the incubation period, the absorbances of the solutions were measured at a wavelength of 517 nm.

2.11 Statistical analysis

The results are presented as the mean ± standard deviation (SD), calculated from a minimum of three independent experiments. Statistical analyses were performed using one-way ANOVA to compare between groups, or two-way ANOVA when interactions between two independent variables were assessed. Before applying ANOVA, we ensured that data met the assumptions of normality and homogeneity of variances. A significance level of $p < 0.05$ was established, denoting a 95% confidence interval for statistical significance. Post hoc analyses, when necessary, were conducted using Tukey's test to control for Type I errors in multiple comparisons. The data were processed and analyzed using statistical software, which was selected for its robustness and wide acceptance in the scientific community. Replicability was reinforced by conducting all experimental conditions in triplicate, ensuring the reliability of the results.

3 Results

3.1 1-DNJ promotes a reduction in cell viability in cancer cell cultures

The compound 1-deoxynojirimycin (1-DNJ) demonstrates a distinct impact on cell viability, revealing differential effects between cancerous and normal cell lines. In the non-neoplastic MRC5 fibroblast cell line, no notable reduction in cell viability was observed at concentrations ranging from 0.5 mM to 18 mM. However, concentrations of 24 mM (0.03% ± 0.003%, $^{***}p \leq 0.0001$, F = 77.14) and 32 mM (0.001%± 0.0017%, $^{***}p \leq 0.0001$, F = 77.14) (refer to Figure 2) exhibited a significant decrease in viability compared to the control. Consequently, the half-maximal inhibitory concentration (IC50) for the MRC5 cell line was determined to be 21.8 mM (R2 = 0.9145, $^{***}p \leq 0.0001$, see Table 1).

In the gastric adenocarcinoma cell line ACP02, 1-DNJ demonstrated a significant reduction in cell viability from 8 mM (82.6% ± 3.13%, $^{***}p \leq 0.0001$, F = 164.3) to 32 mM (5.9% ± 1.06%, $^{***}p \leq 0.0001$, F = 164.3) compared to the control (100% ± 3.21%, $^{***}p \leq 0.0001$, F = 164.3) (see Figure 2). The IC50 for ACP02 was determined to be 19.3 mM, with an IC25 of 9.6 mM (see Figure 2 and Table 1). In the A172 cell line, a significant reduction in viability was observed with 1-DNJ treatment from 6 mM (65.88% ± 6.89%, $^{***}p \leq 0.0001$, F = 144.1) to 32 mM (27.21% ± 1.22%, $^{***}p \leq 0.0001$, F = 144.1) compared to its control (100% ± 6.46%, $^{***}p \leq 0.0001$, F = 144.1). The IC50 for A172 was 5.3 mM, with an IC25 of 2.6 mM, significantly lower than the other cell lines (see Figure 2; Table 1).

The selectivity index of 1-DNJ in A172 and ACP02 cancer cell lines was calculated based on the ratio of their respective IC50 values to the MRC5 normal cell line. A172 exhibited a selectivity index of 4.13, indicating higher selectivity, while ACP02 presented an index of 1.13, suggesting lower selectivity. These results highlight that 1-DNJ demonstrates higher selectivity for the A172 cell line and lacks selectivity for ACP02 by the reference values for the selectivity index, which should be equal to or greater than 3 (see Table 1).

3.2 Treatment with 1-DNJ interferes with the cell cycle of cancer cells

1-DNJ demonstrated an ability to induce a G2/M phase arrest in the A172 cell line at the tested concentrations (Figure 3B) ($^{***}p < 0.0001$) compared to control cultures. Additionally, it exhibited a notable reduction in the number of cells in the G0/G1 phase in the ACP02 cell line (refer to Figure 3A). There was a significant increase in the percentage of ACP02 cells in the G2/M phase by 4.4% ($^{**}p < 0.001$, F = 97.1) and a reduction of 10.95% ($^{***}p < 0.001$, F = 97.1) in the G0/G1 phase at a concentration of 9.6 mM (Figure 3). However, at a concentration of 19.3 mM (refer to Figure 3), an increase of 7.5% ($^{**}p < 0.001$, F = 97.1)

10.3389/fceng.2024.1342755

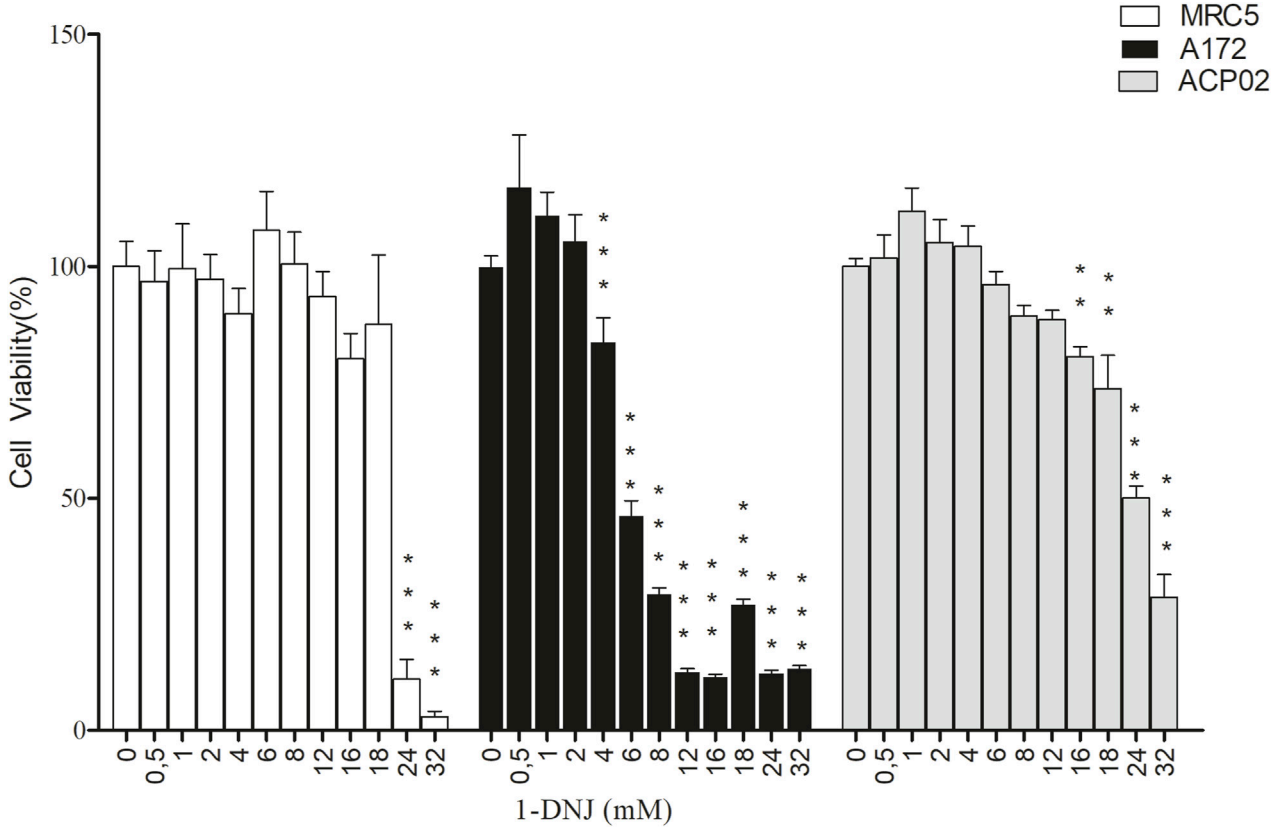

FIGURE 2
Cytotoxic Effects of 1-DNJ on A172, MRC5, and ACP02 Cell Lines In this graph, white bars represent MRC5 cell line, black bars represent A172 cell line, and gray bars represent ACP02 cell line, all treated with concentrations ranging from 0 to 32 mM of 1-DNJ for 72 h. Each data point represents the mean of quadruplicates, and error bars correspond to ±SD. *** p-value <0.0001 or ** p-value <0.001 for the treatment compared to the control (0 mM).

TABLE 1 Maximum inhibitory concentration and selectivity of the isolated substance 1-DNJ in cell lines.

Cell lines	IC50 (mM)	IC25 (mM)	R^2	
MRC5	21.8	10.9	0.953	Selectivity
ACP02	19.3	9.6	0.949	1.13
A172	5.3	2.6	0.952	4.13

MRC5, human normal lung tissue fibroblast lineage; A172, glioblastoma multiforme cell lineage; ACP02, diffuse gastric adenocarcinoma cell lineage.

in cells in the G2/M phase and 3% (*p < 0.05, F = 97.1) in the S phase was observed. Notably, there was also a significant reduction of 18% (***p < 0.001, F = 97.1) of cells in the G0/G1 phase (Figure 3A). In A172 cells (refer to Figure 3B), a percentage of 3.343% (***p < 0.001, F = 99.3) in the G0/G1 phase was observed at a concentration of 2.6 mM (Figure 3) compared to the control without treatment (refer to Figure 3B). At a concentration of 5.3 mM (refer to Figure 3B), there was a reduction in cells in G0/G1 by 4.8% (**p < 0.001, F = 99.3), a decrease of 3.2% (**p < 0.001, F = 99.3) in the S phase, and a relative increase in cells in the G2/M phase by 4.2% (**p < 0.001, F = 99.3), indicating cell cycle arrest in this phase (Figure 3).

3.3 The compound 1-DNJ induces different patterns of cell death in the ACP02 and A172 cell lines

We investigated the impact of 1-DNJ on cell death induction in the ACP02 and A172 cancer cell lines through dual staining with acridine orange and ethidium bromide. The results revealed distinct patterns of cell death induced by the bioactive compound in these cell lines (refer to Figure 4). In the gastric adenocarcinoma cell line ACP02, treatment with 19.3 and 9.6 mM of 1-DNJ for 72 h led to cell death primarily by necrosis, as illustrated in Figure 4A. Necrotic cell death was evident at both concentrations, marked in red within the

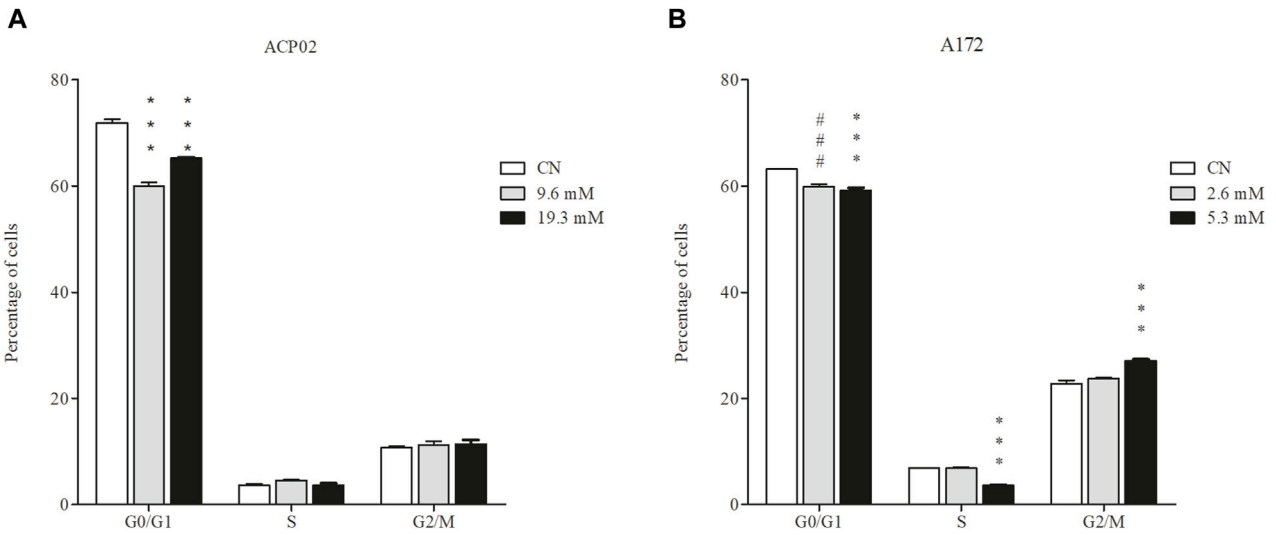

FIGURE 3
Effect of 1-DNJ on the Cell Cycle **(A)** ACP02 cell line treated with concentrations of 9.6 and 19.3 mM of 1-DNJ for 72 h. **(B)** A172 cell line treated with concentrations of 2.6 and 5.3 mM of 1-DNJ. Flow cytometry analysis shows the inhibitory effect of 1-DNJ in blocking the cell cycle at the G2/M phase in the A172 cell line **(B)** and reducing the number of cells in G0/G1 in the ACP02 cell line **(A)** compared to their respective controls. Presented data represent the mean ± standard deviation in quadruplicate. ***p-value <0.0001 vs. corresponding control group and $^{###}p$-value <0.0001 vs. the concentration of 2.6 mM compared to the control.

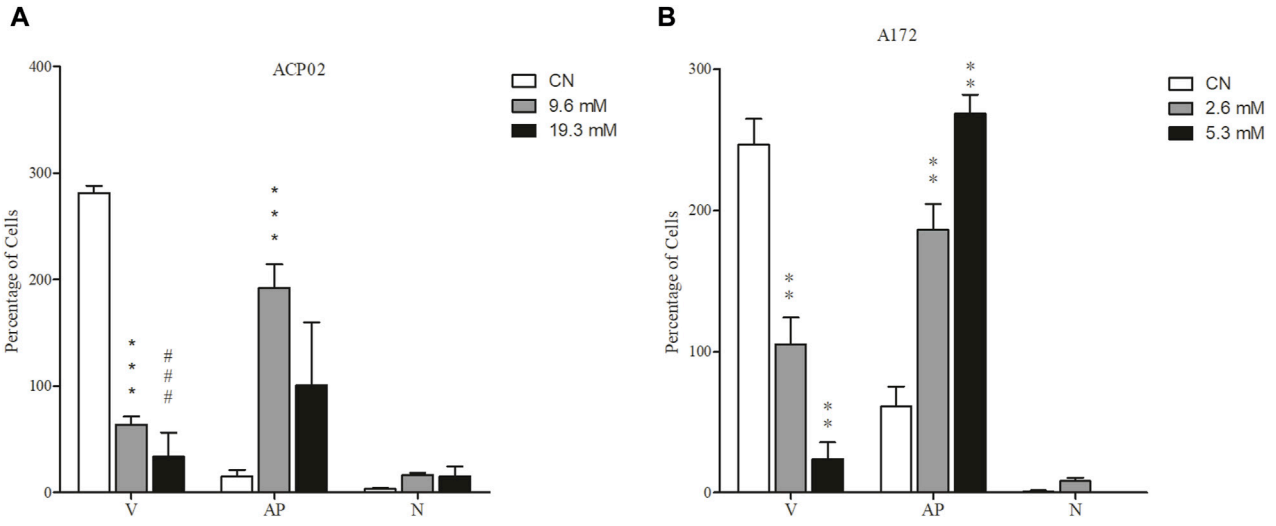

FIGURE 4
1-DNJ Induces Cell Death **(A)** ACP02 cell line treated with concentrations of 9.6 and 19.3 mM of 1-DNJ for 72 h. **(B)** A172 cell line treated with concentrations of 2.6 and 5.3 mM of 1-DNJ. After treatment with 1-DNJ, we observed necrotic cell death (N) in the ACP02 cell line at a concentration of 19.6 mM and apoptosis (AP) in A172 at concentrations of 2.6 and 5.3 mM, compared to their respective controls and the quantity of viable cells (V). Presented data represent the mean ± standard deviation in quadruplicate. ***p-value <0.0001 and $^{###}p$-value <0.0001 vs. the corresponding control group.

cells (Figure 4A). Conversely, in the A172 cell lines (Figure 4B), 1-DNJ induced apoptotic cell death, as indicated by the notable presence of cells marked in orange. Additionally, alterations in cell membrane morphology were observed at both tested concentrations of 2.6 mM and 5.3 mM.

3.4 1-DNJ alters the pattern of cell migration in cell line models

The cancer cell lines underwent treatment with the isolated compound 1-DNJ at various time points (T0, T6, T12, T24, T36, and T48) to evaluate its impact on cellular migration patterns.

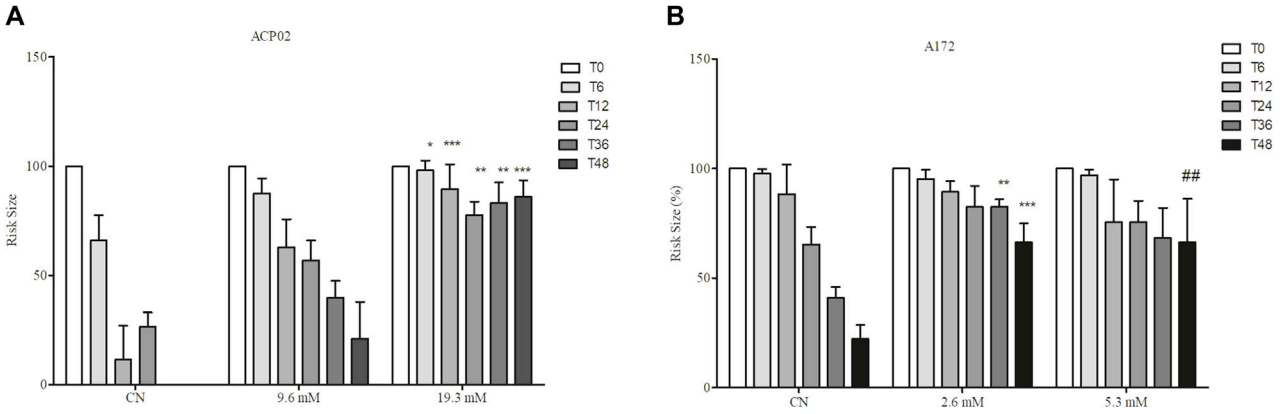

FIGURE 5
Effect of 1-DNJ on the Suppression of Cell Migration in A172 and ACP02 **(A)** ACP02 cell line treated with concentrations of 9.6 and 19.3 mM of 1-DNJ for 72 h. **(B)** A172 cell line treated with concentrations of 2.6 and 5.3 mM of 1-DNJ at time points 0, 6, 12, 24, 36, 48 h (T0 – T48), compared to their respective controls. Presented data represent the mean ± standard deviation in quadruplicate. ***p-value <0.0001 vs. the corresponding control group.

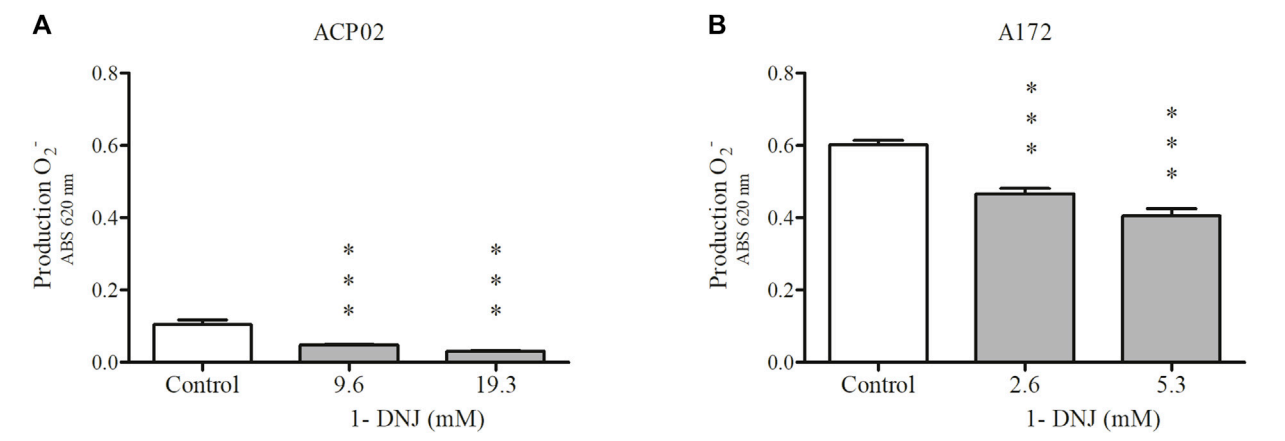

FIGURE 6
1-DNJ Promotes a Reduction in the Production of Superoxide Anion in ACP02 and A172 ACP02 **(A)** treated with 9.6 and 19.3 mM, and A172 **(B)** treated with 2.6 and 5.3 mM, both for 72 h, compared to their respective controls. Presented data represent the mean ± standard deviation in quadruplicate. ***p-value <0.0001 vs. the corresponding control group.

Significant changes in cellular migration were observed in all tested cell lines, but these effects were particularly pronounced at the 48-h time point compared to their respective controls. The concentrations used for ACP02 were 19.3 and 9.6 mM, while those for the A172 cell line were 5.3 and 2.6 mM (Figure 5). In the ACP02 cell line (Figure 5A; Supplementary Material S1), the control demonstrated a decrease in risk over time, signifying normal cell activity in the migration process from 0 h without treatment (100% ± 0.0%, ***$p \leq 0.0001$) to complete closure of the risk at 48 h. This effect was not replicated with 1-DNJ treatment. At 9.6 mM, there was no significant difference compared to the control at 48 h (0.00% ± 0.0%, ***$p \leq 0.0001$), but migration occurred without complete risk closure (21.0% ± 16.0%, *$p \leq 0.005$). At 19.3 mM, a significant difference was observed compared to the control at 48 h (0.00% ± 0.0%, ***$p \leq 0.0001$), and there was no risk area closure (79.5% ± 16.8%, ***$p \leq 0.0001$), indicating that 1-DNJ prevented cellular migration, and this reduction was time-dependent. In the A172 cell line (Figure 5B; Supplementary Material S2), both concentrations of 1-DNJ (2.6 and 5.3 mM) reduced risk size over the 0–48 h of treatment. At 48 h, 2.6 mM (70% ± 10.9%, ***$p \leq 0.0001$) and 5.3 mM (73.5% ± 21.6%, ***$p \leq 0.0001$) showed reduced risk compared to the respective controls at 48 h (22.25% ± 6.29%, ***$p \leq 0.0001$).

3.5 1-DNJ reduces the production of ROS in cancer cell lines

We investigated the potential of 1-DNJ to reduce ROS production in cell lines, using concentrations of 9.6 and 19.3 mM in ACP02 and 2.6 and 5.3 mM in the A172 cell line

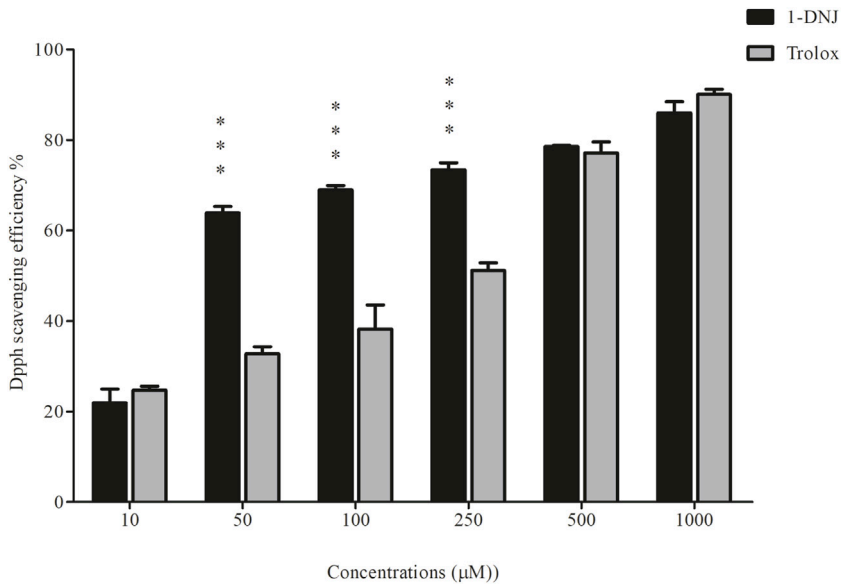

FIGURE 7
1-DNJ Promotes Inhibition of the DPPH· Free Radical Black bars represent the effects of 1-DNJ at different concentrations (10–1,000 μM). Gray bars show the inhibitory capacity of the standard antioxidant trolox against the DPPH radical. Presented data represent the mean ± standard deviation in quadruplicate. ***p-value <0.0001 vs. the corresponding Trolox group.

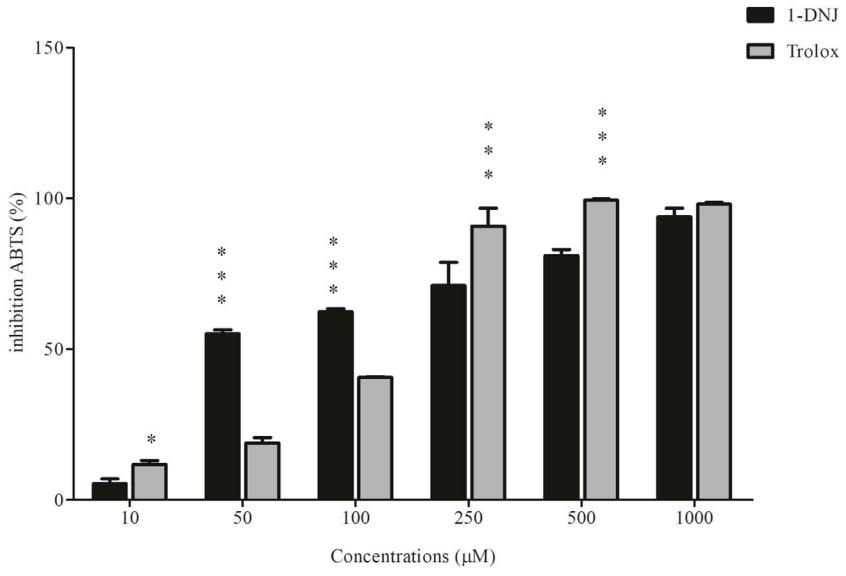

FIGURE 8
1-DNJ Promotes Sequestration of the ABTS Cation Black bars represent the effects of 1-DNJ at different concentrations (10–1,000 μM). Gray bars show the inhibitory capacity of the standard antioxidant trolox against the ABTS cation. Presented data represent the mean ± standard deviation in quadruplicate. ***p-value <0.0001 vs. the corresponding Trolox group.

after a 72-hour treatment period (refer to Figure 6). In the ACP02 cell culture (Figure 6A), the control group exhibited an increase in ROS levels (0.106% ± 0.024%, ***$p \leq 0.0001$). However, following 72 h of treatment with 1-DNJ, a significant reduction in ROS production was observed compared to the ACP02 control cultures at both concentrations, with 9.6 mM (0.048% ± 0.035%, **$p \leq 0.001$) and 19.3 mM (0.03% ± 0.004%, ***$p \leq 0.0001$) (Figure 6A). Similarly, comparable results were observed in the A172 cell line (Figure 6B), where the control showed ROS levels of (0.602% ± 0.02%, ***$p \leq 0.0001$), while the concentrations of

2.6 mM (0.466% ± 0.028%, ***$p \leq 0.0001$) and 5.3 mM (0.405%± 0.039%, ***$p \leq 0.0001$) demonstrated a significant reduction in ROS production. These findings indicate that the A172 cell line, associated with human glioblastoma, also displayed the ability to decrease ROS production upon treatment with 1-DNJ (Figure 6B).

3.6 1-DNJ exhibits antioxidant capacity in cell-free systems

The outcomes of the electron transfer assay employing the DPPH· and ABTS·$^+$ techniques revealed the inhibitory capacity of 1-DNJ against both radicals, surpassing the standard antioxidant Trolox. The results of the DPPH· radical inhibition (Figure 7) indicate that 1-DNJ significantly inhibits the radical at all tested concentrations ranging from 10 to 100 µM, demonstrating a concentration-dependent effect, similar to the Trolox antioxidant. Particularly noteworthy is 1-DNJ's pronounced impact at concentrations of 50 µM (63.85% ± 1.44%, ***$p \leq 0.0001$), 100 µM (68.93% ± 0.98%, ***$p \leq 0.0001$), and 250 µM (73.44% ± 1.51%, ***$p \leq 0.0001$) compared to Trolox at the same concentrations (50 µM: 32.75% ± 0.87%, ***$p \leq 0.0001$; 100 µM: 38.22% ± 5.33%, ***$p \leq 0.0001$; 250 µM: 51.15% ± 1.70%, ***$p \leq 0.0001$) (Figure 7). It suggests that, at these concentrations, 1-DNJ has a higher antioxidant capacity against DPPH radiation. Regarding the ABTS radical (Figure 8), inhibition is observed after interaction with 1-DNJ and Trolox, and this inhibition is also concentration-dependent. However, 1-DNJ continues to display a more significant potential for inhibiting the ABTS radical at concentrations of 50 µM (53.66% ± 1.25%, ***$p \leq 0.0001$) and 100 µM (62.9% ± 1.001%, ***$p \leq 0.0001$) compared to Trolox at 50 µM (19% ± 1.7%, ***$p \leq 0.0001$) and 100 µM (40.58% ± 0.196%, ***$p \leq 0.0001$). It is observed that for this radical, Trolox exhibits a higher potential for inhibition at concentrations of 250 µM (92.54% ± 5.98%, ***$p \leq 0.0001$) and 500 µM (99.21% ± 0.408%, ***$p \leq 0.0001$) compared to 1-DNJ at 250 µM (66.72% ± 7.71%, ***$p \leq 0.0001$) and 500 µM (81.00% ± 2%, ***$p \leq 0.0001$) (Figure 8).

4 Discussion

Cancer remains a significant global health challenge, with conventional treatments often causing systemic side effects due to their non-selective nature (Castedo et al., 2004; Schlichtig et al., 2019; Siegel et al., 2023). In this context, our study explored the potential of 1-deoxynojirimycin (1-DNJ), a compound isolated from wood residue, as a selective anticancer agent in gastric adenocarcinoma and glioblastoma cell cultures.

Our findings demonstrated that 1-DNJ selectively reduces the viability of cancer cells, with a more pronounced effect in glioblastoma cells compared to gastric adenocarcinoma cells. This selectivity is crucial for minimizing cytotoxic effects on healthy cells, as observed in normal cell line MRC5. The cytotoxic and antiproliferative effects of 1-DNJ align with previous studies on natural products, such as N-Alkyl-1,5-dideoxy-1,5-imino-l-fucitols and N-(8-(3-ethynylphenoxy) octyl-1-deoxynojirimycin, which have shown similar effects in various cancer cell lines (Zhao et al., 2010; Zhou et al., 2019; Tang et al., 2020) and show neuroprotective effects (Costa et al., 2021).

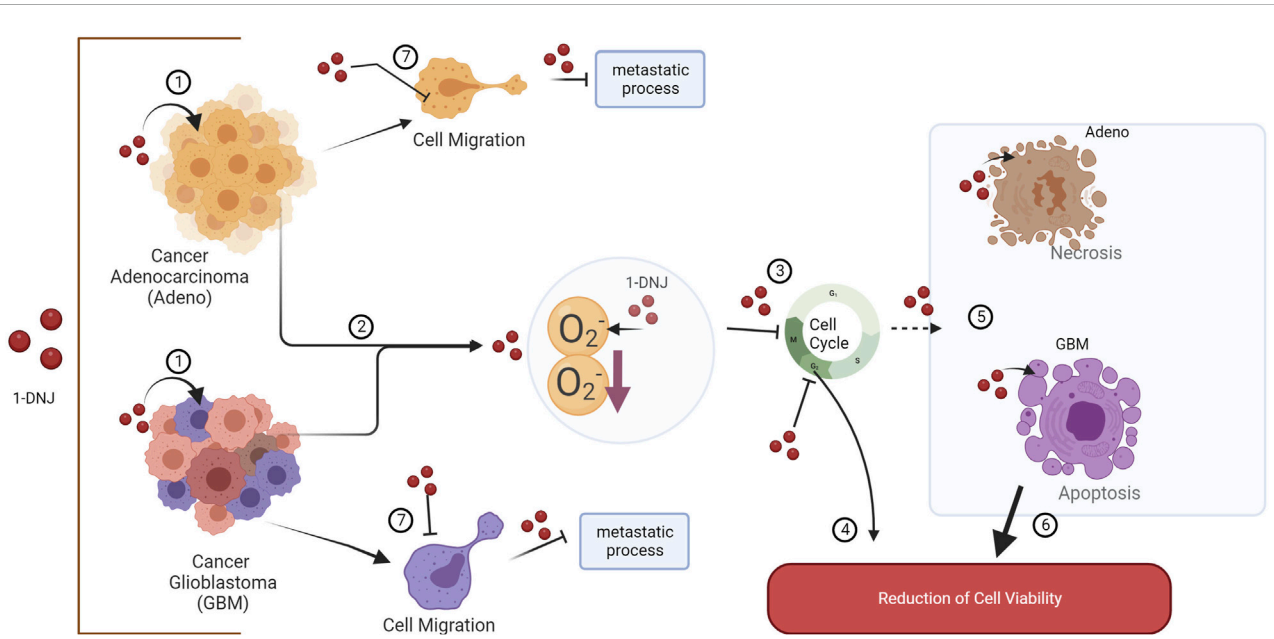

FIGURE 9
Representative Scheme of the Effects of 1-DNJ on A172 and ACP02. (1) 1-DNJ exhibits effects on both gastric adenocarcinoma (Adeno) and glioblastoma multiforme (GBM). (2) 1-DNJ may prevent cancer progression and initiation by reducing superoxide anion and consequently inducing a cell cycle arrest (3) at the G2/M phase in GBM and reducing the number of cells in G0/G1 in Adeno, leading to a decrease in cell viability (4). 1-DNJ also induces cell death in cell lines, such as necrosis in gastric adenocarcinoma and apoptosis in glioblastoma multiforme (5), further contributing to reduced viability (6). Additionally, 1-DNJ alters the cellular migration pattern (7), inhibiting cell motility and the activation of potential pathways that may favor metastatic processes.

4.1 Mechanisms of action and cellular pathways

1-DNJ induced a significant reduction in the production of superoxide anions, suggesting its potential role in modulating oxidative stress, a key factor in cancer progression. The differential production of reactive oxygen species (ROS) in cancer cells is often linked to mitochondrial dysfunction (Zhang et al., 2022), contributing to genomic reprogramming and cancer initiation (Holley et al., 2013; Bronsart et al., 2016; Liberti and Locasale, 2016; Yang et al., 2016). The redox imbalance in tumor cells indicate that manipulating reactive nitrogen and oxygen species as an efficient strategy in cancer therapies (Moloney and Cotter, 2018; Park, 2018). Our results suggest that 1-DNJ may exhibit antioxidant effects, similar to those observed in Morus sp and Broussonetia sp species (Eruygur and Dural, 2019; Cao et al., 2020). These results align with previous data showing the antioxidant capacity of 1-DNJ in inhibiting DPPH• and ABTS•+ radicals through electron transfer and reducing the oxidative potential of these radicals (Rojas-Ocampo et al., 2021). Furthermore, 1-DNJ induced cell cycle arrest in the G2/M phase in glioblastoma cells, a critical phase for DNA replication and mitotic spindle formation. This arrest can lead to DNA damage and activation of cell death pathways, as observed in prostate cancer cells treated with Flavokawain A (Wang et al., 2020). Interestingly, 1-DNJ activated different cell death pathways in the studied cancer cell lines, inducing necrosis in gastric adenocarcinoma cells and apoptosis in glioblastoma cells. This differential response might be linked to the distinct expression of genes associated with tumor aggressiveness and metastatic potential, such as Myc family genes (Barbosa-Jobim et al., 2020; Leal et al., 2009; Valero et al., 2014; Porfírio-Dias et al., 2020).

1-DNJ's influence on cellular pathways extends to its role as an inhibitor of α-glucosidase, a cell surface protein involved in glucose metabolism and insulin signaling (Hatano et al., 2019; Hedrington and Davis, 2019). This inhibition could disrupt cellular signaling pathways, particularly those involved in cancer progression and metastasis, highlighting the potential of 1-DNJ in targeting metabolic pathways in cancer cells (see Figure 9).

4.2 Clinical application and comparison with existing literature**

The selective cytotoxicity and multifaceted mechanisms of action of 1-DNJ position it as a promising candidate for cancer treatment. Its ability to modulate oxidative stress, induce cell cycle arrest, and influence cellular pathways related to glucose metabolism and insulin signaling underscores its potential as a targeted therapy. However, it is crucial to compare these findings with existing literature to understand how they align with or differ from previous research. For instance, the selective cytotoxicity of 1-DNJ in glioblastoma cells compared to gastric adenocarcinoma cells warrants further investigation to elucidate the underlying molecular mechanisms and to explore its potential in treating other cancer types.

4.3 Limitations and future directions**

While our study provides valuable insights into the anticancer potential of 1-DNJ, it is important to acknowledge the limitations of *in vitro* studies. The complex tumor microenvironment and the interactions between cancer cells and their surroundings cannot be fully replicated *in vitro*. Therefore, *in vivo* validation is essential to confirm the efficacy and safety of 1-DNJ in cancer treatment. Further research should also focus on elucidating the molecular mechanisms underlying the differential responses of cancer cells to 1-DNJ treatment and exploring its potential in combination therapies.

In conclusion, 1-DNJ emerges as a promising candidate for cancer therapy, with potential clinical applications in the treatment of gastric adenocarcinoma and glioblastoma. Its selective cytotoxicity, coupled with its ability to modulate cellular pathways involved in cancer progression, warrants further investigation to fully understand its therapeutic potential and to translate these findings into clinical practice.

Data availability statement

The raw data supporting the conclusion of this article will be made available by the authors, without undue reservation.

Ethics statement

Ethical approval was not required for the studies on humans in accordance with the local legislation and institutional requirements because only commercially available established cell lines were used. Ethical approval was not required for the studies on animals in accordance with the local legislation and institutional requirements because only commercially available established cell lines were used.

Author contributions

SF: Conceptualization, Data curation, Formal Analysis, Investigation, Methodology, Supervision, Validation, Writing–original draft, Writing–review and editing. TR: Writing–review and editing. WP: Writing–original draft, Writing–review and editing. ET: Writing–original draft, Writing–review and editing. KdS: Writing–review and editing. MdS: Writing–review and editing. AdS: Writing–original draft, Writing–review and editing. DdV: Writing–original draft, Writing–review and editing. JP: Writing–review and editing. TA: Writing–original draft, Writing–review and editing. AK: Conceptualization, Data curation, Formal Analysis, Funding acquisition, Investigation, Methodology, Project administration, Resources, Supervision, Validation, Writing–original draft, Writing–review and editing. AP: Conceptualization, Data curation, Formal Analysis, Funding acquisition, Investigation, Methodology, Project administration, Resources, Supervision, Validation, Visualization, Writing–original draft, Writing–review and editing.

Funding

The author(s) declare that financial support was received for the research, authorship, and/or publication of this article. SF received a CNPq scholarship. AP received a CNPq fellowship (130058/2020-3). Funds from UFPA/PAPQ covered article processing charges.

Conflict of interest

The authors declare that the research was conducted in the absence of any commercial or financial relationships that could be construed as a potential conflict of interest.

Publisher's note

All claims expressed in this article are solely those of the authors and do not necessarily represent those of their affiliated organizations, or those of the publisher, the editors and the reviewers. Any product that may be evaluated in this article, or claim that may be made by its manufacturer, is not guaranteed or endorsed by the publisher.

Supplementary material

The Supplementary Material for this article can be found online at: https://www.frontiersin.org/articles/10.3389/fceng.2024.1342755/full#supplementary-material

References

Acquah, G. E., Via, B. K., Billor, N., Fasina, O. O., and Eckhardt, L. G. (2016). Identifying plant Part Composition of forest logging residue using infrared spectral data and linear discriminant analysis. *Sensors (Basel)* 16, 1375. doi:10.3390/S16091375

Akar, Z., Küçük, M., and Doğan, H. (2017). A new colorimetric DPPH● scavenging activity method with no need for a spectrophotometer applied on synthetic and natural antioxidants and medicinal herbs. *J. Enzyme Inhib. Med. Chem.* 32, 640–647. doi:10.1080/14756366.2017.1284068

Asner, G. P., Knapp, D. E., Broadbent, E. N., Oliveira, P. J. C., Keller, M., and Silva, J. N. (2005). Ecology: selective logging in the Brazilian Amazon. *Science* 310, 480–482. doi:10.1126/science.1118051

Barbosa-Jobim, G. S., Costa-Lira, É., Ralph, A. C. L., Gregório, L., Lemos, T. L. G., Burbano, R. R., et al. (2020). Biflorin inhibits the proliferation of gastric cancer cells by decreasing MYC expression. *Toxicology in Vitro* 63, 104735. doi:10.1016/j.tiv.2019.104735

Brancalion, P. H. S., Almeida, D. R. A. D., Vidal, E., Molin, P. G., Sontag, V. E., Souza, S. E. X. F., et al. (2018). Fake legal logging in the Brazilian Amazon. *Science Advances* 4. doi:10.1126/SCIADV.AAT1192

Bray, F., Laversanne, M., Weiderpass, E., and Soerjomataram, I. (2021). The ever-increasing importance of cancer as a leading cause of premature death worldwide. *Cancer* 127, 3029–3030. doi:10.1002/CNCR.33587

Bronsart, L. L., Stokes, C., and Contag, C. H. (2016). Multimodality imaging of cancer superoxide anion using the small molecule coelenterazine. *Mol. Imaging Biol.* 18, 166–171. doi:10.1007/S11307-015-0896-7

Cao, X., Yang, L., Xue, Q., Yao, F., Sun, J., Yang, F., et al. (2020). Antioxidant evaluation-guided chemical profiling and structure-activity analysis of leaf extracts from five trees in Broussonetia and Morus (Moraceae). *Sci. Rep.* 10, 4808–4814. doi:10.1038/s41598-020-61709-5

Castedo, M., Perfettini, J. L., Roumier, T., Andreau, K., Medema, R., and Kroemer, G. (2004). Cell death by mitotic catastrophe: a molecular definition. *Oncogene* 23, 2825–2837. doi:10.1038/SJ.ONC.1207528

Costa, T., Fernandez-Villalba, E., Izura, V., Lucas-Ochoa, A., Menezes-Filho, N., Santana, R., et al. (2021). Combined 1-deoxynojirimycin and ibuprofen treatment decreases microglial activation, phagocytosis and dopaminergic degeneration in MPTP-treated mice. *J. Neuroimmune Pharmacol.* 16, 390–402. doi:10.1007/S11481-020-09925-8

Eruygur, N., and Dural, E. (2019). Determination of 1-Deoxynojirimycin by a developed and validated HPLC-FLD method and assessment of In-vitro antioxidant, α-Amylase and α-Glucosidase inhibitory activity in mulberry varieties from Turkey. *Phytomedicine* 53, 234–242. doi:10.1016/J.PHYMED.2018.09.016

George, V. C., Dellaire, G., and Rupasinghe, H. P. V. (2017). Plant flavonoids in cancer chemoprevention: role in genome stability. *J. Nutr. Biochem.* 45, 1–14. doi:10.1016/j.jnutbio.2016.11.007

Hatano, A., Kanno, Y., Kondo, Y., Sunaga, Y., Umezawa, H., and Fukui, K. (2019). Use of a deoxynojirimycin-fluorophore conjugate as a cell-specific imaging probe targeting α-glucosidase on cell membranes. *Bioorg Med. Chem.* 27, 859–864. doi:10.1016/J.BMC.2019.01.032

Hedrington, M. S., and Davis, S. N. (2019). Considerations when using alpha-glucosidase inhibitors in the treatment of type 2 diabetes. *Expert Opin. Pharmacother.* 20, 2229–2235. doi:10.1080/14656566.2019.1672660

Holley, A. K., Dhar, S. K., and Clair, D. K. (2013). Curbing cancer's sweet tooth: is there a role for MnSOD in regulation of the Warburg effect? *Mitochondrion* 13, 170–188. doi:10.1016/J.MITO.2012.07.104

Hyung, S. C., Jun, W. K., Cha, Y. N., and Kim, C. (2006). A quantitative nitroblue tetrazolium assay for determining intracellular superoxide anion production in phagocytic cells. *J. Immunoass. Immunochem.* 27, 31–44. doi:10.1080/15321810500403722

Indrayanto, G., Putra, G. S., and Suhud, F. (2021). Validation of in-vitro bioassay methods: application in herbal drug research. *Profiles Drug Subst. Excip. Relat. Methodol.* 46, 273–307. doi:10.1016/bs.podrm.2020.07.005

Leal, M. F., Martins do Nascimento, J. L., da Silva, C. E. A., Vita Lamarão, M. F., Calcagno, D. Q., Khayat, A. S., et al. (2009). Establishment and conventional cytogenetic characterization of three gastric cancer cell lines. *Cancer Genet. Cytogenet* 195, 85–91. doi:10.1016/J.CANCERGENCYTO.2009.04.020

Lee, H., Jung, D. H., Seo, D. H., Chung, W. H., and Seo, M. J. (2021). Genome analysis of 1-deoxynojirimycin (1-DNJ)-producing Bacillus velezensis K26 and distribution of Bacillus sp. harboring a 1-DNJ biosynthetic gene cluster. *Genomics* 113, 647–653. doi:10.1016/J.YGENO.2020.09.061

Liberti, M. V., and Locasale, J. W. (2016). The warburg effect: how does it benefit cancer cells? *Trends Biochem. Sci.* 41, 211–218. doi:10.1016/J.TIBS.2015.12.001

Marchetti, L., Saviane, A., Montà, A. D., Paglia, G., Pellati, F., Benvenuti, S., et al. (2021). Determination of 1-deoxynojirimycin (1-DNJ) in leaves of Italian or Italy-adapted cultivars of mulberry (Morus sp.pl.) by HPLC-MS. *Plants (Basel)* 10, 1553. doi:10.3390/PLANTS10081553

McDermott, C. L., Irland, L. C., and Pacheco, P. (2015). Forest certification and legality initiatives in the Brazilian Amazon: Lessons for effective and equitable forest governance. *Forest Policy and Economics* 50, 134–142. doi:10.1016/J.FORPOL.2014.05.011

Moloney, J. N., and Cotter, T. G. (2018). ROS signalling in the biology of cancer. *Semin. Cell Dev. Biol.* 80, 50–64. doi:10.1016/J.SEMCDB.2017.05.023

Naik, R., Harmalkar, D. S., Xu, X., Jang, K., and Lee, K. (2015). Bioactive benzofuran derivatives: moracins A-Z in medicinal chemistry. *Eur. J. Med. Chem.* 90, 379–393. doi:10.1016/j.ejmech.2014.11.047

Nyambe, M., Koekemoer, T., van de Venter, M., Goosen, E., and Beukes, D. (2019). *In vitro* evaluation of the phytopharmacological potential of sargassum incisifolium for the treatment of inflammatory bowel diseases. *Medicines* 6, 49. doi:10.3390/medicines6020049

Parida, I. S., Takasu, S., Ito, J., Ikeda, R., Yamagishi, K., Kimura, T., et al. (2019). Physiological effects and organ distribution of Bacillus amyloliquefaciens AS385 culture broth powder containing 1-deoxynojirimycin in C57BL/6J mice. *J. Nutr. Sci. Vitaminol. (Tokyo)* 65, 157–163. doi:10.3177/JNSV.65.157

Park, W. H. (2018). MAPK inhibitors, particularly the JNK inhibitor, increase cell death effects in H2O2-treated lung cancer cells via increased superoxide anion and glutathione depletion. *Oncol. Rep.* 39, 860–870. doi:10.3892/OR.2017.6107

Piao, X., Li, S., Sui, X., Guo, L., Liu, X., Li, H., et al. (2018). 1-Deoxynojirimycin (DNJ) ameliorates indomethacin-induced gastric ulcer in mice by affecting NF-kappaB signaling pathway. *Front. Pharmacol.* 9, 372. doi:10.3389/FPHAR.2018.00372

Pinheiro, W. B. S., Pinheiro Neto, J. R., Botelho, A. S., Dos Santos, K. I. P., Da Silva, G. A., Muribeca, A. J. B., et al. (2022). The use of Bagassa guianensis aubl. forestry waste as an alternative for obtaining bioproducts and bioactive compounds. *Arabian J. Chem.* 15, 103813. doi:10.1016/J.ARABJC.2022.103813

Porfírio-Dias, C. L., Melo, K. M., Bastos, C. E. M. C., Ferreira, T. A. A., Azevedo, L. F. C., Salgado, H. L., et al. (2020). Andiroba oil (Carapa guianensisAubl) shows cytotoxicity but no mutagenicity in the ACPP02 gastric cancer cell line. *J. Appl. Toxicol.* 40, 1060–1066. doi:10.1002/JAT.3966

Rojas-Ocampo, E., Torrejón-Valqui, L., Muñóz-Astecker, L. D., Medina-Mendoza, M., Mori-Mestanza, D., and Castro-Alayo, E. M. (2021). Antioxidant capacity, total

phenolic content and phenolic compounds of pulp and bagasse of four Peruvian berries. *Heliyon* 7, e07787. doi:10.1016/J.HELIYON.2021.E07787

Schlichtig, K., Dürr, P., Dörje, F., and Fromm, M. F. (2019). New oral anti-cancer drugs and medication safety. *Dtsch. Arztebl Int.* 116, 775–782. doi:10.3238/ARZTEBL.2019.0775

Shahrestanaki, M. K., Bagheri, M., Ghanadian, M., Aghaei, M., and Jafari, S. M. (2019). Centaurea cyanus extracted 13-O-acetylsolstitialin A decrease Bax/Bcl-2 ratio and expression of cyclin D1/Cdk-4 to induce apoptosis and cell cycle arrest in MCF-7 and MDA-MB-231 breast cancer cell lines. *Journal of Cellular Biochemistry*. doi:10.1002/jcb.29141

Siegel, R. L., Miller, K. D., Wagle, N. S., and Jemal, A. (2023). Cancer statistics, 2023. *CA Cancer J. Clin.* 73, 17–48. doi:10.3322/CAAC.21763

Sridhar, K., and Charles, A. L. (2019). *In vitro* antioxidant activity of Kyoho grape extracts in DPPH and ABTS assays: estimation methods for EC50 using advanced statistical programs. *Food Chem.* 275, 41–49. doi:10.1016/J.FOODCHEM.2018.09.040

Sung, H., Ferlay, J., Siegel, R. L., Laversanne, M., Soerjomataram, I., Jemal, A., et al. (2021). Global cancer statistics 2020: GLOBOCAN estimates of incidence and mortality worldwide for 36 cancers in 185 countries. *CA Cancer J. Clin.* 71, 209–249. doi:10.3322/caac.21660

Tang, Q., Xia, H., Liang, W., Huo, X., and Wei, X. (2020). Synthesis and characterization of zinc oxide nanoparticles from Morus nigra and its anticancer activity of AGS gastric cancer cells. *J. Photochem Photobiol. B* 202, 111698. doi:10.1016/J.JPHOTOBIOL.2019.111698

Turan, I., Demir, S., Kilinc, K., Burnaz, N. A., Yaman, S. O., Akbulut, K., et al. (2017). Antiproliferative and apoptotic effect of Morus nigra extract on human prostate cancer cells. *Saudi Pharm. J. SPJ* 25, 241–248. doi:10.1016/J.JSPS.2016.06.002

Valero, M. L., Cimas, F. J., Arias, L., Melgar-Rojas, P., García, E., Callejas-Valera, J. L., et al. (2014). E1a promotes c-Myc-dependent replicative stress: implications in glioblastoma radiosensitization. *Cell Cycle* 13, 52–61. doi:10.4161/CC.26754

Wang, K., Zhang, W., Wang, Z., Gao, M., Wang, X., Han, W., et al. (2020). Flavokawain A inhibits prostate cancer cells by inducing cell cycle arrest and cell apoptosis and regulating the glutamine metabolism pathway. *J. Pharm. Biomed. Anal.* 186, 113288. doi:10.1016/J.JPBA.2020.113288

Watanabe, C., Naveed, N., and Neittaanmäki, P. (2018). Digital solutions transform the forest-based bioeconomy into a digital platform industry - a suggestion for a disruptive business model in the digital economy. *Technology in Society* 54, 168–188. doi:10.1016/J.TECHSOC.2018.05.002

Yang, Y., Karakhanova, S., Hartwig, W., D'Haese, J. G., Philippov, P. P., Werner, J., et al. (2016). Mitochondria and mitochondrial ROS in cancer: novel targets for anticancer therapy. *J. Cell Physiol.* 231, 2570–2581. doi:10.1002/JCP.25349

Yatsunami, K., Ichida, M., and Onodera, S. (2008). The relationship between 1-deoxynojirimycin content and α-glucosidase inhibitory activity in leaves of 276 mulberry cultivars (Morus spp.) in Kyoto, Japan. *J. Nat. Med.* 62, 63–66. doi:10.1007/S11418-007-0185-0

Yin, H., Shi, X. Q., Sun, B., Ye, J. J., Duan, Z. A., Zhou, X. L., et al. (2010). Accumulation of 1-deoxynojirimycin in silkworm, *Bombyx mori* L. *J. Zhejiang Univ. Sci. B* 11, 286–291. doi:10.1631/JZUS.B0900344

Zhang, B., Pan, C., Feng, C., Yan, C., Yu, Y., Chen, Z., et al. (2022). Role of mitochondrial reactive oxygen species in homeostasis regulation. *Redox Rep.* 27, 45–52. doi:10.1080/13510002.2022.2046423

Zhao, Y., Liu, W., Zhou, Y., Zhang, X., and Murphy, P. V. (2010). N-8-(3-ethynylphenoxy) octyl-1-deoxynojirimycin suppresses growth and migration of human lung cancer cells. *Bioorg Med. Chem. Lett.* 20, 7540–7543. doi:10.1016/J.BMCL.2010.09.065

Zhou, J., Negi, A., Mirallai, S. I., Warta, R., Herold-Mende, C., Carty, M. P., et al. (2019). N-Alkyl-1,5-dideoxy-1,5-imino-l-fucitols as fucosidase inhibitors: synthesis, molecular modelling and activity against cancer cell lines. *Bioorg Chem.* 84, 418–433. doi:10.1016/J.BIOORG.2018.12.003